Reviewers' comments:

Reviewer #1 (Remarks to the Author):

In this manuscript, the authors described a surface enhanced Raman spectroscopy (SERS) approach to monitor pH on cell surfaces with a relatively high spatial resolution. AuNPs modified with 4-mercaptobenzoic acid (4-MBA) were conjugated on cell surfaces using the biotin-streptavidin interaction. The monolayer of 4-MBA on AuNPs has strong surface plasmon enhanced Raman scattering, and the scattering depends on the pH of the surrounding nanoenvironment, enabling the sensing of local pH on cell surfaces. This study represents a new application of cell membrane modification and is of interest to the field. The developed method may be useful to reveal some fundamental biological questions. However, there are several major issues need to be addressed.

1. Figure 2c-d showed nice ring like structures, indicating Alexa-streptavidin was on the cell membranes. However, the fragmentation of nuclei may be an indicator of cell apoptosis. The data raise a concern on the viability of cells after the treatment. The authors claimed that the modification did not induce cell death, but there is no any cell viability data in the main text or supporting information.
2. In this study, cell membranes were first biotinylated and conjugated with biotinylated AuNPs using streptavidin as the bridge. The same method has been previously developed for anchoring NPs on cell membranes (Cheng et al. ACS Nano, 2010, 4, 625), in which some data may be used as references for works presented in this manuscript. A review paper (Stephan et al. Nano Today, 2011, 6, 309.) may be helpful for the authors to learn more about engineering cell surfaces with NPs. The authors have claimed that their AuNPs stayed on cell surfaces without detectable internalization by MKN28 cells. It is important to describe clearly the time frame of the study because NPs cannot stay on cell surfaces forever. To explain the low NP uptake, the authors mentioned that "the sulfo group in the molecular label prevented endocytosis" on page 5 without citing any references. Even if the free linker molecule is cell membrane-impermeable, it cannot explain the low endocytosis of AuNPs at here because the endocytosis of AuNPs likely depends on the cell membrane proteins that AuNPs linked to. In the previous paper of Cheng et al, it was explained that the multiple binding of NPs with cell membranes interfered with cell endocytosis and caused NP aggregation on cell membranes.
3. To conjugate AuNPs on cell membranes, streptavidin was attached on bionylated AuNPs, but leaving some biotin sites available. The authors then biotinylated cell membranes and coated another layer of streptavidin on cells before conjugating AuNPs on cell surfaces. The rationale of this complicated process is unclear. Why don't directly conjugate streptavidin-coated AuNPs on biotinylated cell membranes or directly conjugate biotinylated AuNPs on streptavidin-coated cell surfaces?
4. The authors have used the term pH nanosensor. However, the resolution of SERS signal was about 1 um as shown in Figure 7. The 2D SERS signal itself cannot directly distinguish protons in cytosol of cells and on cell membranes. It relies on the navigation of AuNPs via other methods. Compared to a recent publication utilizing surface energy transfer to AuNPs for local intracellular pH detection (ACS Nano DOI: 10.1021/acsnano.8b02200), the approach described in this manuscript does not seem have advantages in spatial resolution or convenience for broad applications. Note the method in this very recent ACS Nano paper can be extended to membrane-conjugated AuNPs.
5. Figure 7c studied the change of average pH value on cell surfaces with and without the presence of EIPA. To further validate the strategy, an established method detecting the pH variation caused by EIPA should be used as a control.
6. The TEM images in Figure 4 clearly showed AuNP aggregation and a heterogeneous distribution on cell surfaces. It is unclear if the local SERS signal difference is due to pH variation on cell surfaces or the difference of local AuNP density. An experiment needs to be designed to address this question. For example, fixing the cells after AuNP conjugation on cell surfaces may eliminate local pH difference. Can the SERS signal become homogeneous?

Reviewer #2 (Remarks to the Author):

In this work, authors reported a method for interstitial pH sensing with high resolution based on SERS. Specifically, they immobilized the gold nanoparticles (AuNPs), which are functionalized with 4-mercaptobenzoic acid (4-MBA), to the cell membrane via a streptavidin bridge using two molecular compounds containing biotin: a pyridyldithiol-biotin compound (HPDP-B), which conjugates to AuNP via thiol-gold interaction, and a sulfo-NHS-ester-biotin compound (NHS-B) that reacts with the primary amines of lysine and the amino-termini of polypeptides on the outer cell membrane surface. Since the SERS signal of the COO- band varies with pH values due to protonation/de-protonation, the relative peak intensity change is used to indicate the pH values after obtaining the calibration curve. Using 4-MBA functionalized SERS-active substrates (either AuNPs (refs 19-22) or Au nanostructures (e.g., Biosensors and Bioelectronics 73 (2015) 202–207) for cell pH sensing have been reported. From this point of view, this method is not new. The unique of this work lies on the using of NHS-B to un-specifically link to membrane proteins and then using streptavidin to further link HPDP-B to 4-MBA functionalized AuNPs. In this way, AuNPs are located at the outside of cell membrane close to ion channels and transporters, enabling pH sensing locally and even after treated with NHE inhibitor, while AuNPs are located in the intracellular in the previous reported works (refs. 19-22). However, the work (Biosensors and Bioelectronics 73 (2015) 202–207) reported the direct and accurate mapping extracellular pH of living cells in complex media using SERS based on 4-MBA functionalized Au nanostructure arrays. Therefore, in general, the work is an increment, lacks of novelty. In addition, more comments are provided below.

1. The assignment of 1068 and 1588 cm-1 peaks in the sentence on P.6 line 207 is wrong, i.e., "…bands located at 1068 and 1588 cm-1 are due to v8a and v12 aromatic ring vibrations, respectively,…" The bands located at 1068 and 1588 cm-1 should be due to v12 and v8a aromatic ring vibrations, respectively. Therefore, the sentence on p. 7 line 229 "…v8a or v12 aromatic ring vibrations, namely bands C+H or D+I in Fig. 5 (a),…" is also wrong.

2. The assignment and explanation about 1390 and 1415 cm-1 bands could also be questionable. In the work reported in Biosensors and Bioelectronics 73 (2015) 202–207, it showed the peak intensity change of two peaks versus the pH values from 4.05 to 8.99. In that work, Au nanostructure instead of AuNPs was used as the SERS-active substrates, so there is less or no chance for $-MBA molecules that have form SAM to undergo a dramatic orientation change.

3. Caption of Figure 5a should provide the ratio of 4-MBA/HPDP-B. The 2-pyridine shown in Figs. 5a and 5b could cause a confusion as there is no 2-pyridine was immobilized on AuNPs. Why are the four strong peaks shown in Fig. 5b due to HPDP-B related to 2-pyridine? Due to the smaller Raman scattering cross-section of HPDP-B compared to 4-MBA, it is reasonable that the intensity is about one order of magnitude lower than 4-MBA in Fig. 5a. The four strong peaks in Fig. 5b should be more related to O=C-NH as they are more close to sensing surface.

4. As reported in Biosensors and Bioelectronics 73 (2015) 202–207, other cations, especially divalent cations (Ca2+, Mg2+) can cause the intensity change and the peak shift of ~1420 cm-1 peak. In this study, as stated on p.11 lines 358-361, "During the spectroscopic analyses we used an isotonic buffer solution containing 115 mM NaCl, 15 mM NaNO3, 5 mM KCl, 1 mM Ca(NO3)2 , 1 mM Mg(NO3)2, 10 mM HEPES, 10 mM glucose, 10 mM sucrose and adjusted to pH 7.4 by adding CsOH." Therefore, the calibration curve (Fig. 6a) should also be done in such solution. While this won't affect the trend by adding EIPA, the real pH values could be different.

5. The 2D pH mapping via the xy raster scan shown in Figure 7 should provide the z position. As

shown in Figure 2 of Supporting Information, SERS spectra signal only appeared locally where AuNP aggregations are. Also, for Figure 2 of Supporting Information, it also needs to indicate where this z-scan was done. My guess is that this should not be in the middle of the cell as the strong SERS signal from the middle of the z-scan range. This z-scan might be taken close to the edge of the cell.

6. The claim of two peaks at 999 and 1021 cm-1, which are associated with the decomposed aromatic species (i.e., TP), needs to be careful. Why there are no obvious such two peaks in the pH calibration experiments, i.e., Figure 6, for both acidic (pH = 6.0) and basic (pH = 8.0), compared to the detection of cells (Fig. 7)? The increase of these two peaks could be due to the orientation change of 4-MBA. The increase of these two peaks upon the binding of fructose on 4-mercaptobroic acid SAM was reported in ACS Nano 9, 2668 (2015).

7. In the Figure 3 of Supporting Information, the optical images show clearly that there are many AuNPs at the edges of cells. Did authors collect the SERS data from those areas? How about the pH values of those areas?

8. CFM was applied to confirm the label was only at the membrane of cells. However, as shown in TEM and even optical images, the AuNPs can be clearly seen. Therefore, CFM method may not be needed.

9. Figure 1 of Supporting Information needs to provide the z values for each line scan.

10. The wavenumber of peak around 1600-1670 cm-1 was labeled differently in the Figure 7 caption (1063 cm-1) but 1068 cm-1 in the legend.

Reviewer #3 (Remarks to the Author):

In the present article a novel method (or approach) that aims to measure the extremely sharp pH gradients in extracellular environments, close to cell mebrane proteins, is deveoped. This is a a topic of great relevance in Cell Biology due to its critical role in controlling many celular functions, including cell proliferation, metastasis, drug resistance and apoptosis.
The method consist in anchoring Au nanoparticles (NPs) functionalized with a mercaptobenzoic acid (MBA) to the outer part of the cell membrane. As the MBA molecule is known to be a molecule whose Raman response is dependent on the external pH, a calibration curve that relates the ratio between typical Raman bands of this molecule and the pH could be constructed. The presence of Au NPs provides an enhancement of the Raman signals of MBA (SERS) as well as a method to localize them only on the extracelular membrane region.

This attachment is achieved by treating the membrane with a sulfo-NHS-ester-biotin compound which reacts specifically with the polypeptides present in the membrane and by functionaling the Au NP also with a pyridyldithiol-biotin compound (HPDP-B), and then adding Streptavidin (STV) that acts as a bridge between the biotinylated Au NP and the biotinylated cell membrane.

At the same time control confocal fluorescence microscopy (using STV with a flourescence probe molecule) experiments, as well as TEM images, demosntrate the succesful functionalization of the external part of the cell membrane.

All the experiments were performed with human gastric adenocarcinoma cell line, MKN28, and the shape of Au NPs (nano-urchins) was chosen to maximize the SERS enhancement of the MBA molecule.

The nanometer size of the AuNP sensor attached to the proteins and the use of SERS allows to visualize the highly localized variation of pH induced by proton extrusion, which is upregulated in cancer cells. The measurements were performed
before and after addition of ethyl-isopropyl amiloride (EIPA), an inhibitor of $Na+/H+$ exchanger (NHE). In addition Raman image was also performed for scanning (using the MBA molecule as reporter) the ph variation along the z direction.

The article is well written and of great interest for a wide audience , however it seems to me that the following issues shoud be addressed, before the manuscript should be suitable to be published in Nature communications:

a) For the calibration curve, the SERS active modes coming from HPDP B and TP molecules seems to be taken into account. However in the real samples also the Raman bands of Streptavidine should experience significant SERS enhancement.
Have the authors considered this issue?.

b) The resolution of the average pH measurements are difraction limited to the size of the laser spot, therefore the SERS signals are the average within this area and also the
pH values. It is not clear why the axial resolution is difraction limited while the resolution along the other directions is dictated by the size of the Au NP degree of agglomeration. This point should be explained more clearly.

c) Can the author estimate the SERS enhancement factor of the relevant molecular probe involved (MBA) and its dependence on the degree of Au NP agglomeration. This issue is very important since the value of pH depends on the SERS intensity of the relevant bands and their intensities should also depend on the degree of agglomeration and the average distance between Au NPs.

Response to the Reviewers' comments and remarks:

We sincerely thank the Reviewers for their time and effort in reviewing our paper. Independently on the final result of this submission, we would like to express our appreciation and gratitude for the extremely valuable and pertinent comments to our research. We strongly believe that the Reviewers' remarks and opinions highly contributed to improve the quality of our work after thoughtful and careful revision. In the revised version of the manuscript, we addressed all the queries raised by the Reviewers, point by point. In addition, new data are also presented to elevate the quality of our study, which is now much more detailed and comprehensive. We are confident that the new compelling experimental evidence and discussion will remove any doubt over our statement of unprecedented method for cell surface pH measurement based on surface enhanced Raman spectroscopy. The revised parts in the new manuscript and the answers to each comment in this document are written in red:

Reviewer #1 (Remarks to the Author):

1. Figure 2c-d showed nice ring like structures, indicating Alexa-streptavidin was on the cell membranes. However, the fragmentation of nuclei may be an indicator of cell apoptosis. The data raise a concern on the viability of cells after the treatment. The authors claimed that the modification did not induce cell death, but there is no any cell viability data in the main text or supporting information.

In the revised manuscript we provide cell viability data (MTT assay and propidium iodide (PI) fluorescent staining) as requested by the Reviewer. Please refer to the new text added at the end of the section *Outer cell membrane surface labelling* (pg. 6, starting from "As a final validation step of the protocol,...); the new Fig. 4 and the details of the protocol at pg. 18, in the paragraph *Cytotoxicity assay* of the section *Methods*. We acknowledge the importance of this information that was missing. Please note that Fig. 2 of the original manuscript is Fig. S1 in the revised manuscript (it was moved to *Supporting information*). We would like to remark the fact that in Figs. S1 (e)-(g) nuclear fragmentation can be observed in two cells that are in the final stage of mitosis, during which nuclear fragmentation is a physiological feature. In order to substantiate this point, we also provide new fluorescence images obtained from MKN-28 cells stained with PI and Hoechst dyes, in which there are clear examples of mitosis with nuclei fragmentation and without PI red fluorescence. Please refer to Figs. (f)-(i). We believe that the presented new images represent a further validation of the cell viability test results, namely the lack of cell apoptosis induced by our treatment.

2. In this study, cell membranes were first biotinylated and conjugated with biotinylated AuNPs using streptavidin as the bridge. The same method has been previously developed for anchoring NPs on cell membranes (Cheng et al. ACS Nano, 2010, 4, 625), in which some data may be used as references for works presented in this manuscript. A review paper (Stephan et al. Nano Today, 2011, 6, 309.) may be helpful for the authors to learn more about engineering cell surfaces with NPs. The authors have claimed that their AuNPs stayed on cell surfaces without detectable internalization by MKN28 cells. It is important to describe clearly the time frame of the study because NPs cannot stay on cell surfaces forever. To explain the low NP uptake, the authors mentioned that "the sulfo group in the molecular label prevented endocytosis" on page 5 without citing any references. Even if the free linker molecule is cell membrane-impermeable, it cannot explain the low endocytosis of AuNPs at here because the endocytosis of AuNPs likely depends on the cell membrane proteins that AuNPs linked to. In the previous paper of Cheng et al, it was explained that the multiple binding of NPs with cell membranes interfered with cell endocytosis and caused NP aggregation on cell membranes.

We thank Reviewer #1 for the interesting comment and suggestions. We referred the work by Chen et. al. at pg. 4, Line 6 from the bottom *(Ref.* [28]). We humbly admit that we were not aware of that work and we believe that the previous use of NHS-biotin for unspecific labeling of surface proteins with Neutravidin conjugated nano-fluorospheres should be mentioned, but it does not diminish the novelty of our pH sensor. In fact, the basic idea of our method has a different purpose and, consequently, the strategy for nanoparticles conjugation and attachment is more elaborated. The use of NHS-biotin and streptavidin (SA) is only one piece of a more complex puzzle that had to be carefully assembled to achieve the final goal of attachment

55 AND pH measurement. The AuNP surface cannot be entirely conjugated with SA as reported by Chen et. al.
56 because the SERS intensity from SA should not interfere with the 4-MBA signal. For this reason, we firstly
57 conjugated SA to the NHS-biotin attached to the outer membrane proteins and then with added the AuNPs
58 functionalized with 4-MBA and HPDP-biotin. The result is approximatively 1 SA for 1 AuNP and,
59 consequently, the effect of this protein to the collected SERS signal is negligible. For the same reason, also
60 the concentration of HPDP-biotin bound to AuNP had to be adjusted to avoid contribution to the collected
61 SERS intensity. The result of this calibrated procedure is the homogeneous distribution of AuNP showed in
62 our paper and the formation of nanoclusters. We believe that these arguments require to be clearly elucidated
63 in the revised manuscript and we took advantage of the Reviewer's comment to implement the text at the
64 beginning of paragraph *Outer cell membrane surface labelling* at pg. 4. As far as the AuNP internalization
65 issue is concerned, when we mention that "the sulfo group in the molecular label prevented endocytosis" on
66 page 5, we are referring to the previous Fig. 2 (now S1 of *Supporting information*), which reports the results
67 of cell surface biotinylation without AuNP. In fact, the experiments with sulfo-NHS-biotin conjugated with
68 fluorescent dye (i.e., without AuNPs) were designed to study the reaction of NHS ester group to the cell
69 membrane proteins. In cancer cells we found that higher pH of the buffer solution during 30 minutes of
70 biotinylation increased the yield of reaction. These experiments also confirmed the homogeneous distribution
71 of sulfo-NHS-biotin molecules attached to the cell surface. The presence of the sulfo-group prevents
72 internalization of NHS-biotin and enables only the selective targeting of cell outer membrane proteins. Once
73 the AuNP are attached to NHS-biotin after the following step of the protocol, we are completely aware that
74 the endocytosis of AuNP is not prevented by the sulfo-groups. We apologize for the improper use of
75 "endocytosis" in the phrase mentioned by the Reviewer, which may have been misleading. In the revised
76 manuscript we changed the word "endocytosis" to "internalization", which is referred only to NHS-biotin
77 during the biotinylation step (see pg. 5, 7th line from the bottom of the page). The lack of AuNP endocytosis
78 during our Raman experiments was proved by the results showed in Fig. 3 (i.e., Fig. 4 of the previous
79 version): the TEM images were purposely taken from cells that underwent to fixation 1 hour after the end of
80 AuNP attachment, which corresponds to the average time spent for the Raman experiments shown in this
81 paper. In the original manuscript, at Line 19 of pg. 5, we stated that we waited 1 hr before fixation and TEM
82 imaging. Cheng et al. showed lack of endocytosis for up to 2 days, which is a remarkable result that was
83 explained by nanoparticles binding with multiple surface proteins. In the revised version we added this
84 explanation in the new text from Line 7 of pg. 6. In addition, Reference [30] (Stephan et al. Nano Today,
85 2011, 6, 309) was added at pg. 6, Line 13.

87 3. To conjugate AuNPs on cell membranes, streptavidin was attached on bionylated AuNPs, but leaving
88 some biotin sites available. The authors then biotinylated cell membranes and coated another layer of
89 streptavidin on cells before conjugating AuNPs on cell surfaces. The rationale of this complicated process is
90 unclear. Why don't directly conjugate streptavidin-coated AuNPs on biotinylated cell membranes or directly
91 conjugate biotinylated AuNPs on streptavidin-coated cell surfaces?
92 Actually, we directly conjugated biotinylated AuNPs to streptavidin-coated cell surfaces. In the paragraph
93 *Conjugation of AuNP for SERS and CFM analyses* of the section *Method*, we did not mention any incubation
94 of AuNP with SA. The nanoparticles are conjugated with 4-MBA and HPDP-biotin. In the paragraph
95 *Protocol for cell membrane surface labelling with conjugated AuNP* we explained 3 separated steps: 1)
96 NHS-Biotin reacting with cell surface proteins; 2) washing and addition of SA that reacts with NHS-biotin;
97 3) washing and incubation with 4-MBA/HPDP-biotin conjugated AuNP. Please see the new text at the
98 beginning of paragraph *Outer cell membrane surface labelling* (pg. 4), as also already discussed in the
99 answer to Comment 2.
100 In the case of CFM experiments, we conjugated AuNP with streptavidin-Alexa488 in order to attach the
101 fluorescent dye to some of the HPDP-biotin previously attached to the AuNP. The HPDP-biotin:streptavidin-
102 Alexa488 ratio was 3:2, in order to leave unreacted biotins on the surface of AuNPs for the attachment to
103 surface membrane proteins coated with streptavidin.

105 4. The authors have used the term pH nanosensor. However, the resolution of SERS signal was about 1 μm
106 as shown in Figure 7. The 2D SERS signal itself cannot directly distinguish protons in cytosol of cells and on
107 cell membranes. It relies on the navigation of AuNPs via other methods. Compared to a recent publication
108 utilizing surface energy transfer to AuNPs for local intracellular pH detection (ACS Nano DOI:
109 10.1021/acsnano.8b02200), the approach described in this manuscript does not seem have advantages in

spatial resolution or convenience for broad applications. Note the method in this very recent ACS Nano paper can be extended to membrane-conjugated AuNPs.

We believe that the Reviewer is referring to 1 µm as the in-plane resolution. The in-plane resolution is given by the size of the laser spot, which is diffraction limited and it was estimated as 700 nm (See the new Fig. 3 (b) in the revised manuscript). Note that in the original version we erroneously reported the FWHM of the Gaussian beam (441 nm). We repeated more experiments with fluorescent beads and we used the width of the Gaussian function at $1/e^2$ of its peak, which is a better estimation of the spot size (now 700 nm). In Fig. 8 (Fig. 7 of the original manuscript), we show the results of in-plane xy raster scans of points with 1 µm steps, in which the pH value of each point is associated to the relative 1 µm × 1 µm square of the mesh. This is an approximation for graphical purposes. In reality, each colored square of the map should be reshaped as a circle and scaled down to a diameter of 0.7 µm. We added to the caption of Fig. 8 that each point of the maps corresponds effectively to a spot of 700 nm diameter. We hope that we may be granted of this graphical approximation. Nonetheless, for the scope of the present investigation, which is the highly localized measurement of cell outer surface pH, the spatial resolution that matters the most is the one given by the distance of the sensor from the cell outer surface and the size of the sensor itself. According to our results, the nanoparticles are clearly attached to the outer surface and the size of the sensor ranges from 90 nm (1 AuNP) to 400 nm (biggest observed nano-aggregates). In other words, the size and the location of the pH-probe are suitable to investigate the layer of the extracellular milieu in which steep pH gradients manifest themselves. Please refer to the new text at pg. 6, from Line 16. See also the answer to Comment 2 of Reviewer #3.

We added new text in the *Conclusion*, at pgs. 13 and 14, in which we mention the interesting method introduced in ACS Nano DOI: 10.1021/acsnano.8b02200. The pH assessment based on surface energy transfer using gold nanoparticles and fluorescence dyes reduces the rates of laser-induced photo-bleaching in multi-hour live-cell experiments. This method can certainly be extended to cell outer membrane surface analysis, by taking advantage of part of the knowledge introduced in our paper. Nonetheless, the spatial resolution will be equal to our SERS-based method, as well as the "time window" in which extracellular surface pH can be reliably measured, which is controlled by the endocytosis of the AuNP.

5. Figure 7c studied the change of average pH value on cell surfaces with and without the presence of EIPA. To further validate the strategy, an established method detecting the pH variation caused by EIPA should be used as a control.

We provided standard measurement of cytosolic pH variation induced by EIPA during the acute phase using pH-sensitive fluorescent dye. Although these pH data are not comparable to the highly localized measurements of surface pH, the drop of intracellular pH during the acute phase confirm the inhibition of Na^+/H^+ exchangers and the rise of external surface pH measured by SERS. See the new Fig. S7 in *Supporting information*; the text at pg. 12, from Line 8 and the experimental procedure added in paragraph *Confocal fluorescence microscopy* at pg. 16.

6. The TEM images in Figure 4 clearly showed AuNP aggregation and a heterogeneous distribution on cell surfaces. It is unclear if the local SERS signal difference is due to pH variation on cell surfaces or the difference of local AuNP density. An experiment needs to be designed to address this question. For example, fixing the cells after AuNP conjugation on cell surfaces may eliminate local pH difference. Can the SERS signal become homogeneous?

We performed the requested experiment and the data were added in the new Fig. 8 of the revised version, which presents the results of 4 cases: MKN-28 with and without addition of EIPA; HepG2 with and without addition of glutaraldehyde/paraformaldehyde for fixation. Please refer to pg. 12, from Line 12, where new text was added to introduce the new data of Fig. 8 (d).

Reviewer #2 (Remarks to the Author):

Using 4-MBA functionalized SERS-active substrates (either AuNPs (refs 19-22) or Au nanostructures (e.g., Biosensors and Bioelectronics 73 (2015) 202–207) for cell pH sensing have been reported. From this point of view, this method is not new. The unique of this work lies on the using of NHS-B to un-specifically link to membrane proteins and then using streptavidin to further link HPDP-B to 4-MBA functionalized AuNPs. In

166 this way, AuNPs are located at the outside of cell membrane close to ion channels and transporters, enabling
167 pH sensing locally and even after treated with NHE inhibitor, while AuNPs are located in the intracellular in
168 the previous reported works (refs. 19-22). However, the work (Biosensors and Bioelectronics 73 (2015) 202–
169 207) reported the direct and accurate mapping extracellular pH of living cells in complex media using SERS
170 based on 4-MBA functionalized Au nanostructure arrays. Therefore, in general, the work is an increment,
171 lacks of novelty.
172 We were aware of that paper, but we believe that the spatial resolution of our method can be compared to
173 that reported by Anderson et al. (Ref. [12]), which, on the other hand, can be applied only to cancer cells
174 because based on the use of low-pH insertion peptides and it may be limited by photo-bleaching of the
175 fluorescent dye. The method proposed in *Biosensors and Bioelectronics 73 (2015) 202–207)* by Sun *et.al.* is
176 certainly remarkable. It enabled to visualize surface acidosis in HepG2 liver cancer cells, but the mean value
177 of pH was 7.2, namely much more alkaline than those reported in previous investigations on extracellular pH
178 of solid hepatocellular carcinomas (see Ref [19-21] and the text added in the introduction at pg. 3 and 4).
179 Accordingly, if the pH-sensitive probe on the substrate of Sun *et al.* had been indeed entirely attached to the
180 cell surface, it should have detected higher proton concentration. In the revised paper, we present new data
181 collected from HepG2 using our method. Cell surface pH was estimated as 6.7, much more acidic than pH
182 reported by *Sun et. al.*. Please refer to the new Fig. 8. In the manuscript, starting from the last two lines of pg.
183 12, we address this issue. We explain that HepG2 cells exhibit high concentration of filopodial protrusions
184 formed on the membrane (see Ref. [55, 56]). The TEM image in Fig. 3 (a) of our revised manuscript clearly
185 shows the presence of micrometric filopodia also on the basal surface of MKN-28 cells. From this
186 morphological characterization it follows that in Sun *et. al.* the cells adhered to the gold nanostructured
187 substrate through filopodia, while an extended part of 4-MBA SAM probed by the laser was "untouched",
188 but separated at micrometric distance from the membrane, where the effect of the buffer solution affected the
189 pH results. In addition, the method reported by Sun *et. al.* can be applied only to study the basal side of the
190 cells, while in our method the nanoparticles can be attached to both apical and basolateral side of cells,
191 which may be important for future studies on epithelial cells. The pores of permeable membranes for
192 epithelial cell culture enable the biotinylation of the basolateral surface and the attachment of nanoparticles
193 (we are currently making experiments on human bronchial epithelial cells). Based on these considerations,
194 we believe that the difference between the two methods is obvious, not only in terms of experimental
195 approach but, by far, in terms of enhanced spatial resolution and localization of the surface pH assessment.
196 For this reason we did not add the paper of Sun *et al.* to the discussion of the previous manuscript that was
197 originally conceived as a short communication. We regret about that choice because we now acknowledge
198 that supplemental experimental evidence and discussion concerning this issue were necessary.
199 We hope that these new evidence and arguments may convince the Reviewer to reconsider her/his previous
200 opinion about lack of novelty in our work.
201
202
203 1. The assignment of 1068 and 1588 cm-1 peaks in the sentence on P.6 line 207 is wrong, i.e., "…bands
204 located at 1068 and 1588 cm-1 are due to ν8a and ν12 aromatic ring vibrations, respectively,…" The bands
205 located at 1068 and 1588 cm-1 should be due to ν12 and ν8a aromatic ring vibrations, respectively.
206 Therefore, the sentence on p. 7 line 229 "…ν8a or ν12 aromatic ring vibrations, namely bands C+H or D+I in
207 Fig. 5 (a),.." is also wrong.
208 The Reviewer is correct and we thank him/her for noticing our careless mistake. See the corrections at pg. 8,
209 Line 20 and pg. 10, Line 2.
210
211 2. The assignment and explanation about 1390 and 1415 cm^{-1} bands could also be questionable. In the work
212 reported in Biosensors and Bioelectronics 73 (2015) 202–207, it showed the peak intensity change of two
213 peaks versus the pH values from 4.05 to 8.99. In that work, Au nanostructure instead of AuNPs was used as
214 the SERS-active substrates, so there is less or no chance for 4-MBA molecules that have form SAM to
215 undergo a dramatic orientation change.
216 In Biosensors and Bioelectronics 73 (2015) 202–207 (hereafter referred to Ref. [18], as in the revised
217 manuscript), the COO$^-$ symmetric stretching was studied considering only one band, whose increase of
218 intensity due to increasing pH was noticed along with the peak shift toward higher frequencies. The observed
219 shift was attributed to some 4-MBA molecules involved in hydrogen bonding and to the possible interaction
220 between COO$^-$ groups and the ring hydrogens, but the clear asymmetric nature of this band at neutral and
221 alkaline pH was neglected.

222 In the revised manuscript, we decided to mention also the explanation of the shift proposed in Ref. [18],
223 based on hydrogen bonding. Nonetheless, we also keep the characterization of band shift and the formation
224 of a clear shoulder band according to our original interpretation, which was suggested also by Michiota et al.
225 [Ref. 33]. We added Ref. [35], in which calculation based on density functional theory on the adsorption
226 behavior of 4-MBA on silver colloids demonstrated that, depending on pH, the protonated molecules are
227 bonded to the metal surface only through the S atoms, while, in the deprotonated form, through the S atoms
228 and the COO^- groups with a tilted orientation, causing significant intensity shift and the onset of a shoulder
229 band. Moreover, we added Ref. [36], which demonstrated that benzoic acid, in which thiol group is not
230 present, conjugates to gold substrates via carboxylate group and the COO^- symmetric stretching band is
231 centered at around 1370 cm^{-1}, namely gold surface can interact with COO^-, inducing massive shift of the
232 Raman stretching band to lower frequencies. Please refer to the new text added from the first line of pg. 8.
233 Independently on which of the two explanations is more plausible, we believe that the deconvolution of the
234 Raman intensity around 1400 cm^{-1} with 2 bands is the most correct approach. In fact, this approach considers
235 the contribution of every COO^- group forming the SAM, namely it is more accurate. Also in Fig. 3 (a) of Ref.
236 [18] it is clear that, at alkaline pH, the band peak shifts to higher frequencies, but also a shoulder at lower
237 frequency is formed. The frequencies of the shoulder sub-band are the same frequencies of the band at more
238 acidic pH, namely the sub-band is still associated to −COO^- stretching. Nonetheless, this shoulder was
239 neglected in pH calculation of previous studies.

240

241 3. Caption of Figure 5a should provide the ratio of 4-MBA/HPDP-B. The 2-pyridine shown in Figs. 5a and
242 5b could cause a confusion as there is no 2-pyridine was immobilized on AuNPs. Why are the four strong
243 peaks shown in Fig. 5b due to HPDP-B related to 2-pyridine? Due to the smaller Raman scattering cross-
244 section of HPDP-B compared to 4-MBA, it is reasonable that the intensity is about one order of magnitude
245 lower than 4-MBA in Fig. 5a. The four strong peaks in Fig. 5b should be more related to O=C-NH as they
246 are more close to sensing surface.
247 We added the ratio of 4-MBA/HPDP-B in the new Fig. 5 (a) and in its caption.
248 In addition, we reported a new spectrum of HPDP-B in Fig. 5 (b), from AuNP colloidal solution conjugated
249 with higher concentration of HPDP-B, which was equal to the concentration used for 4-MBA in Fig. 5(a).
250 In the previous version we showed the spectrum at low concentration, which is the HPDP-B concentration
251 used for conjugation of the pH-sensor. The aim of the previous version was the confirmation of HPDP-B
252 conjugation at low concentration and its negligible Raman signal as compared to 4-MBA SAM signal. In the
253 new version, the HPDP-B spectrum is more intense and the detailed characterization of the SAM is possible.
254 In Fig. S3 of *Supporting information*, we show the HPDP-B spectrum compared to the SERS spectrum of 2-
255 pyridine thiolate. The assignments are reported in Table S1 of *supporting information*.
256 The HPDP-B molecule is composed of a pyridyldithiol group linked to a biotin residue via a 2.9 nm hexyl
257 arm spacer. The disulfide bridge reacts with the gold surface, leading to dissociative adsorption of HPDP-B
258 through gold-adatom-mediated bonds as 2-pyridine (2-Py) thiolate and biotin-hexyl spacer arm thiolate.
259 We did not detect the S-S stretching band at around 500-515 cm^{-1}, namely the disulfide bond was broken as
260 expected (i.e., we added also new references [37] and [38]). The most intense bands of 2-Py thiolate are also
261 observed in the HPDP-B spectrum, since this molecule is close to the sensing surface. In the HPDP-B
262 spectrum, we also observed other less intense bands that were associated to the biotin-hexyl spacer arm
263 thiolate. Please refer to the new text added from Line 23 of pg. 8.

264

265

266

267 4. As reported in Biosensors and Bioelectronics 73 (2015) 202–207, other cations, especially divalent cations
268 ($Ca2+$, $Mg2+$) can cause the intensity change and the peak shift of ~1420 cm-1 peak. In this study, as stated
269 on p.11 lines 358-361, "During the spectroscopic analyses we used an isotonic buffer solution containing 115
270 mM NaCl, 15 mM NaNO3, 5 mM KCl, 1 mM Ca(NO3)2 , 1 mM Mg(NO3)2, 10 mM HEPES, 10 mM
271 glucose, 10 mM sucrose and adjusted to pH 7.4 by adding CsOH." Therefore, the calibration curve (Fig. 6a)
272 should also be done in such solution. While this won't affect the trend by adding EIPA, the real pH values
273 could be different.
274 The reviewer is absolutely right and we thank her/him. We repeated the calibration with AuNP in isotonic
275 buffer solutions at different pH. The new calibration is shown in the new Fig. 7(a). The divalent cations
276 clearly affected the band ratio, similarly to Biosensors and Bioelectronics 73 (2015) 202–207 (Ref. [18]).
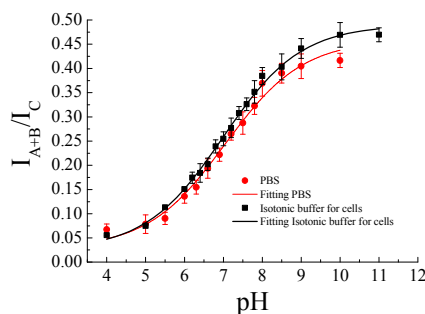
280
281
282　Accordingly, we recalculated the pH values on the surface of the analyzed cells. The results are shown in the
283　new Fig. 8. Please note that the cell surface pH values in MKN28 with and without EIPA are now about 0.2
284　lower than those reported in the original manuscript. The new results are certainly more accurate and they
285　can finally be compared to those obtained in Ref [12] in the case of cancer cells in the presence of glucose,
286　as in our experiments. In facts, in our results based on the previous calibration, the MKN28 surface was more
287　acidic than the cancer cells of Ref. [12] analyzed without glucose, but more alkaline than the cancer cells of
288　Ref. [12] with glucose. Since in our buffer solution we had glucose, we are happy that our corrected results
289　are more consistent with the previous results of Ref. [12]. Please refer to the new Fig. 8 and the correction
290　from Line 17 of pg. 13.
291
292　5. The 2D pH mapping via the xy raster scan shown in Figure 7 should provide the z position. As shown in
293　Figure 2 of Supporting Information, SERS spectra signal only appeared locally where AuNP aggregations
294　are. Also, for Figure 2 of Supporting Information, it also needs to indicate where this z-scan was done. My
295　guess is that this should not be in the middle of the cell as the strong SERS signal from the middle of the z-
296　scan range. This z-scan might be taken close to the edge of the cell.
297
298　Please refer to the new explanation added from Line 4 from the bottom of pg. 10. The *z*-coordinate of each *x*-
299　*y* raster scan was set after estimation of the average AuNP position in the middle of each analyzed cell by *z*-
300　*axis* line scans. Considering the micrometric axial length of the laser probe, this procedure enabled to
301　illuminate the AuNP attached to the surface in the majority of the investigated spots. The axial length of the
302　laser probe was showed in the new Fig. S5 in *Supporting information*.
303　The scan in Fig. 2 of *Supporting information* in the previous version is now modified for clarity sake and
304　reported in the new Fig. S4 of *Supporting information*. We apologize for the lack of clarity in the explanation
305　that may have confused the Reviewer. The scan was performed in the middle of the cell. It is a *z-scan*, from
306　the bottom glass upon which the cell was seeded to 20 μm above the bottom glass, across the cell. The
307　position of the maximum intensity at *z*=12 μm is the location of the AuNP, namely the cell membrane, since
308　we demonstrated that AuNP are attached to the outer cell surface. In the new Fig. S4, we added a sketch of
309　the cell cross-section along which the *z-axis* line scan of Raman spectra was collected. We added in the
310　caption of Fig. S4 that the *z-axis* line scan was performed in the middle of the cell.
311
312
313　6. The claim of two peaks at 999 and 1021 cm-1, which are associated with the decomposed aromatic species
314　(i.e., TP), needs to be careful. Why there are no obvious such two peaks in the pH calibration experiments,
315　i.e., Figure 6, for both acidic (pH = 6.0) and basic (pH = 8.0), compared to the detection of cells (Fig. 7)?
316　The increase of these two peaks could be due to the orientation change of 4-MBA. The increase of these two
317　peaks upon the binding of fructose on 4-mercaptobroic acid SAM was reported in ACS Nano 9, 2668 (2015).
318
319　In Fig. 6 of the original manuscript, we purposely selected two spectra at different pH but similar lack of
320　transformation. The aim of the figure is to emphasize the variation of the intensities A+B and E as a function
321　of pH. For this purpose, we found appropriate to choose two spectra with similar but marginal onset of F, G,
322　H, and I bands. Please consider that, at laser power of 20 mW, in colloidal solutions we did not detect

spectral transformation in every measurement. In the new manuscript we added new arguments and new experiments to validate our theory of SAM transformation. Please refer to Fig. 6 and the discussion from Line 12 of pg. 9. The power of the laser indisputably effected the transformation, which was not observed in every measurement obtained with 1mW (note that in Ref. [18], for example, transformation was not observed because they used 1 mW). At maximum power (i.e., 72 mW) we always observed the onset of F, G, H, and I bands. The positions of the new bands, as well as the ratios of their intensities, clearly resemble the spectrum of TP shown in Fig. 5 (c). Nonetheless, we mentioned also the interpretation of Sun *et. al.* (Ref. [46]). As suggested by the Reviewer, they hypothesized that the origin of these bands in 4-mercaptophenylboronic acid (4MPBA) affected by fructose may be due to reorientation and charge redistribution of the benzene ring. Conversely, Ly et al. (doi.org/10.1002/sia.6184) observed deboronation reaction of 4MPBA via fructose and glucose on silver surfaces by SERS at the excitation wavelengths of 488, 514, and 633 nm. They found all the characteristic bands of TP as we did. The new Fig. 6 (h) demonstrates that, although we can debate the origin of the new bands, when they are observed, the deconvolution in sub-bands and the use of band C is essential for precise pH calculation.

7. In the Figure 3 of Supporting Information, the optical images show clearly that there are many AuNPs at the edges of cells. Did authors collect the SERS data from those areas? How about the pH values of those areas?

Please refer to the new text at pg. 11, from Line 18. We also prepared a new Fig. S6 in *Supporting information*. The average pH measured from spectra of micro-aggregations is 7.41. An example of spectra collected from micro-aggregation is showed in Fig. S6 (a). In Fig. S6 (b), we compared the intensities of Band C collected from micro-aggregations, colloidal solutions and x-y raster scans on the surface of cells without micro-aggregations. There is a clear difference between the intensities detected on micro-aggregations and the investigated cell surfaces.

8. CFM was applied to confirm the label was only at the membrane of cells. However, as shown in TEM and even optical images, the AuNPs can be clearly seen. Therefore, CFM method may not be needed.

We moved Fig. 2 of the previous version to the *Supporting information* (Fig. S1). We would like to preserve Fig. 3 of the previous version, which is now Fig. 2 in the revised version. The TEM images confirm the AuNP attachment on the outer membrane, but Fig. 3 is useful to prove the distribution of the AuNP on the cell surface (*xy plane*).

9. Figure 1 of Supporting Information needs to provide the z values for each line scan.

We added the information as requested. Figure 1 of Supporting Information is Fig. S2 in the *Supporting information* of the revised manuscript.

10. The wavenumber of peak around 1600-1670 cm-1 was labeled differently in the Figure 7 caption (1063 cm-1) but 1068 cm-1 in the legend.

Thank you for noticing this careless mistake. Figure 7 is now Fig. 8 and the caption was modified to explain the new implemented figure and to fix the mistake (i.e., 1068 instead of 1063).

Reviewer #3 (Remarks to the Author):

1. For the calibration curve, the SERS active modes coming from HPDP B and TP molecules seems to be taken into account. However in the real samples also the Raman bands of Streptavidin should experience significant SERS enhancement. Have the authors considered this issue?

According to our protocol, streptavidin (SA) first reacts with biotinylated surface proteins; then, only after removal of unreacted SA, we add the functionalized AuNP to the cell sample. The AuNP were separately conjugated to 4-MBA and HPDP-B. This is a crucial feature of the experimental method, since it guarantees that each AuNP attached to the cell membrane has approximately only one SA molecule close to its surface, namely the SERS signal of SA does not affect the overriding signal of the pH-sensitive 4-MBA self-assembled monolayer (SAM). In addition, the Raman scattering is not enhanced in every location of the gold

377 surface, but only on the surface of some hot spots. The hot spots are concentrated on the tips of the nano-
378 urchins and in the gap between two adjacent AuNP in a nano-cluster. Moreover, the enhancement decreases
379 exponentially from the surface (i.e., max) to about 10-15 nm away from the surface (i.e., negligible
380 enhancement). The small 4-MBA is adsorbed on the surface and the SAM is only 0.78 nm thick (Ref. [30]).
381 Conversely, the SA attached to AuNP is some nanometer away from the surface, considering the HPDP-B
382 arm spacer length of 3.9 nm. In summary, i) the ratio between 4-MBA and SA on the gold surface is
383 massively in favor of 4-MBA; ii) the probability that SA is located in the hot spot is also small; iii) the
384 enhancement factor on the SA attached to gold is smaller than the enhancement on the 4-MBA molecules
385 stuck on the surface. Please refer to the new text at pg. 4, Line 6 from the bottom.
386

387 2. The resolution of the average pH measurements are diffraction limited to the size of the laser spot,
388 therefore the SERS signals are the average within this area and also the pH values. It is not clear why the
389 axial resolution is diffraction limited while the resolution along the other directions is dictated by the size of
390 the Au NP degree of agglomeration. This point should be explained more clearly.

391
392 We added new explanation of the spatial resolution at pg. 6, from Line 16. In the new Fig. 3 (b) we also
393 added an explanatory description of the SERS pH-probe given by the interaction between the laser beam and
394 the AuNP. The in-plane spatial resolution of the measurement can be approximated as the size of the laser
395 spot. Conversely, we define the axial resolution as the maximum distance from the cell surface at which the
396 pH is measured. Since the SERS signal is merely originated from the 4-MBA SAM (i.e., 0.78 nm thickness,
397 depicted with green lines in Fig. 3(b)) the axial resolution can be approximated as the size of the nano-
398 sensors. For example, if we consider one approximatively spherical AuNP attached to the surface, it can
399 probe pH as close as in the point of attachment and as far as in the diametrically opposite point of the AuNP.
400 The pH calculated by SERS is approximately the average. See the following sketch:
401
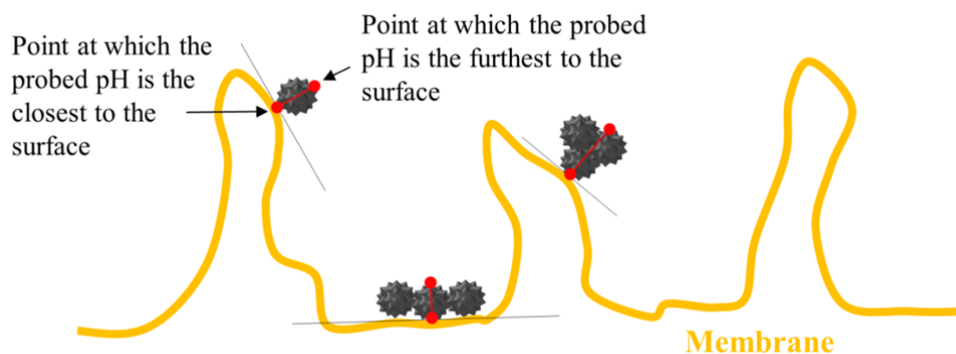
402
403

404 3. Can the author estimate the SERS enhancement factor of the relevant molecular probe involved (MBA)
405 and its dependence on the degree of Au NP agglomeration. This issue is very important since the value of pH
406 depends on the SERS intensity of the relevant bands and their intensities should also depend on the degree of
407 agglomeration and the average distance between Au NPs.

408 We thank the reviewer for the suggestion. We calculated the enhancement factor. See the new text at the end
409 of the paragraph *Measurement of pH using AuNP and SERS* (pg. 10); the details of the calculation in the
410 paragraph *Enhancement factor calculation* of the section *Methods* (pgs. 17 and 18) and the new Fig. S9.
411
412
413 ADDITIONAL INFORMATION FROM THE AUTHORS:
414
415 Figure S8 of *Supporting information* is the modified version of the previous Fig. 3 of *Supporting information*.
416 We show now 4 additional examples of hyperspectral maps of surface pH from MKN28, HepG2 and
417 MKN28 treated with EIPA.

Reviewers' comments:

Reviewer #1 (Remarks to the Author):

The authors have addressed all my questions. The quality of this manuscript has been significantly improved. However, one concern of this manuscript is still the resolution limit, which is not better than existing pH detection methods.

Reviewer #2 (Remarks to the Author):

In the revision, authors carried out more experiments and revised the manuscript carefully to address the reviewer's comments. While the quality of the work has been significantly improved, some discussions need to be careful to avoid misleading.

1. Regarding the answer to the second question, the reviewer would suggest the authors pay attention to the following points. (a) The condition that the 4-MBA SAM is formed. In both refs 33 and 35, the 4-MBA SAMs were formed in AUEQOUS solution under different pH values. No doubt, under alkaline condition in aqueous solution, COOH groups are deprotonated, so FREE 4-MBA molecules can adsorb on Au (Ag) surface via thiol to form S-Au(Ag) bond and via COO- to form COO-Au(Ag) bond. As pointed in ref. 35, under acidic and neutral conditions (in aqueous solution), 4-MBA adsorb on Ag via strong Ag-S bond, while weak COO-Ag and S-Ag in alkaline condition. In this work, the 4-MBA SAM was formed in PBS buffer condition according to the experimental description. So, majority of 4-MBA (if not all) should adsorb on Au surface via strong Au-S bond. In ref. 18, however, the 4-MBA SAM was formed in ethanol solution, so the binding should be Au-S. (b) Once the 4-MBA SAM has been formed via the Au-S bond, all the 4-MBA molecules have been anchored on the Au surface. In this work, after forming 4-MBA and HPDP-B SAM, "the Au NPs were collected after centrifugation and resuspended in PBS at pH 7.4 for cells treatment or in isotonic buffer solution at different pH for the calibration of the nanosensor (i.e., in the pH range 4 to 10)." So, the COOH group (unbounded) will be protonated or deprotonated in response to the solution / environment pH change. Two possible situations could cause COO-Au interaction even though SAM has been formed: (i) two gold nanoparticles are very close (could be the case in this work since TEM images show Au NP clusters, but this should not be the case when authors did pH calibration in bulk solution), but this is still rare given each NP already has a SAM layer; (ii) multilayer 4-MBA formed in the SAM forming procedure as pointed in ref. 35 (and other people also reported that multilayer instead of monolayer could be formed). In this case, the outer layer 4-MBA molecules that are deprotonated in alkaline condition could diffuse to Au surface and bind via COO-Au bond. Taking these two points into account, the sentences starting with "On the other hand..." in redline on p. 8 lines 256-264 could be misleading. In short, when 4-MBA molecules are free in aqueous solution, under alkaline condition, they can form S-Au and COO-Au bond, but once the SAM has been formed via Au-S, these already bounded molecules have no option to form COO-Au bond even under alkaline condition. The fact of asymmetric peak around 1400 cm-1 was definitely observed in many publications (like ref. 22 as well). It for sure needs more investigation. Nonetheless, the reviewer feels the discussion on p. 8 lines 256-264 could be misleading.
2. Based on authors' assignment of 1370 cm-1 peak due to COO-Au, then these COO are not free, they can't respond to pH change, then they should not be counted in the intensity ratio (I_A+B/I_C) for the calibration curve. Did authors try to plot the calibration curve using I_B/I_C?

Reviewer #3 (Remarks to the Author):

In this revised version of the manuscript the authors have performed significant improvements clarifying in a satisfactory way all the main issues pointed out by myself. In this respect they have clarified the important feature concerning the spatial resolution of the pH sensor and have also analysed the relevant

reporter molecules that are used for pH estimation as well as performed an estimation of the SERS enhancemnet factor (lower bound).

Therefore, I consider that the main concerns have adequately been answered and the manuscript is now suitable for publication in Nature Communications

Response to Reviewers' remarks:

We truly appreciated the Reviewers' comments, opinions and support to prepare a revised version of our manuscript. We would like to thank the 3 Reviewers for the valuable time they have spent reviewing our work. The revised parts in the new manuscript and the answers to each comment in this document are written in red:

Reviewer #1 (Remarks to the Author):

The authors have addressed all my questions. The quality of this manuscript has been significantly improved. However, one concern of this manuscript is still the resolution limit, which is not better than existing pH detection methods.

In the first revision of the manuscript we addressed the issue of the spatial resolution. In the previously revised manuscript, we acknowledged that pH assessment based on surface energy transfer using gold nanoparticles and fluorescence dyes has similar spatial resolution of our method. Nonetheless, the use of this technique for the measurement of extracellular pH on the outer surface of the cells has not yet been exploited and published. In addition, the use of this technique should take advantage of part of the knowledge presented in our paper to effectively attach the pH-sensor to the outer membrane. We amply discussed in the manuscript the method based on low-pH insertion peptides, which has been thoroughly compared to our method. In conclusion, as compared to other techniques that have similar spatial resolution, we would like to remark that our experimental procedure can be implemented in a simple and nimble way, since the cell preparation before Raman analysis requires only a couple of hours. The method was purposely developed using commercially available materials, which are easy to find. In addition to ex-vivo analysis, it has the potential to combine in-vivo cell sorting for diagnostic purpose and phototherapy: in fact, a calibrated increase of power output in the micrometric laser focus induces cell death due to the highly localized heat generated on the gold metal surface. At the completion of the surgical procedure, the nanoparticles attached to the healthy tissue may be washed away, since they are attached to the external membrane without endocytosis and the bonds are cleavable. Obviously, this future potential application of the technique has to be carefully evaluated, developed and tested to prove to be effective. Nowadays, the use of advanced spectrometer for tissue imaging combined to data discrimination by machine learning-based cell classifiers is gaining more and more popularity. Hopefully, such interest will foster the fast improvement and refinement of the technique. In light of these considerations, we hope that the manuscript may be worthy of publication in Nature Communications.

Reviewer #2 (Remarks to the Author):

In the revision, authors carried out more experiments and revised the manuscript carefully to address the reviewer's comments. While the quality of the work has been significantly improved, some discussions need to be careful to avoid misleading.

1.   Regarding the answer to the second question, the reviewer would suggest the authors pay attention to the following points. (a) The condition that the 4-MBA SAM is formed. In both refs 33 and 35, the 4-MBA SAMs were formed in AUEQOUS solution under different pH values. No doubt, under alkaline condition in aqueous solution, COOH groups are deprotonated, so FREE 4-MBA molecules can adsorb on Au (Ag) surface via thiol to form S-Au(Ag) bond and via COO- to form COO-Au(Ag) bond. As pointed in ref. 35, under acidic and neutral conditions (in aqueous solution), 4-MBA adsorb on Ag via strong Ag-S bond, while weak COO-Ag and S-Ag in alkaline condition. In this work, the 4-MBA SAM was formed in PBS buffer condition according to the experimental description. So, majority of 4-MBA (if not all) should adsorb on Au surface via strong Au-S bond. In ref. 18, however, the 4-MBA SAM was formed in ethanol solution, so the binding should be Au-S. (b) Once the 4-MBA SAM has been formed via the Au-S bond, all the 4-MBA

molecules have been anchored on the Au surface. In this work, after forming 4-MBA and HPDP-B SAM, "the Au NPs were collected after centrifugation and resuspended in PBS at pH 7.4 for cells treatment or in isotonic buffer solution at different pH for the calibration of the nanosensor (i.e., in the pH range 4 to 10)." So, the COOH group (unbounded) will be protonated or deprotonated in response to the solution / environment pH change. Two possible situations could cause COO-Au interaction even though SAM has been formed: (i) two gold nanoparticles are very close (could be the case in this work since TEM images show Au NP clusters, but this should not be the case when authors did pH calibration in bulk solution), but this is still rare given each NP already has a SAM layer; (ii) multilayer 4-MBA formed in the SAM forming procedure as pointed in ref. 35 (and other people also reported that multilayer instead of monolayer could be formed). In this case, the outer layer 4-MBA molecules that are deprotonated in alkaline condition could diffuse to Au surface and bind via COO-Au bond. Taking these two points into account, the sentences starting with "On the other hand…" in redline on p. 8 lines 256-264 could be misleading. In short, when 4-MBA molecules are free in aqueous solution, under alkaline condition, they can form S-Au and COO-Au bond, but once the SAM has been formed via Au-S, these already bounded molecules have no option to form COO-Au bond even under alkaline condition. The fact of asymmetric peak around 1400 cm^{-1} was definitely observed in many publications (like ref. 22 as well). It for sure needs more investigation. Nonetheless, the reviewer feels the discussion on p. 8 lines 256-264 could be misleading.

The comment and suggestion from the Reviewer are correct and pertinent. We agree that, once the SAM is formed by thiol adsorption, the variation of pH did not lead to "molecular flip-flop" associated to COO$^-$ adsorption on the gold surface. In the first revised manuscript, we hypothesized that the SERS intensity of band A at around 1390 cm^{-1} may be due to S-Au bonded deprotonated molecules in which the carboxylate groups interact with the metal surface. References 33, 35 and 36 of the previously revised manuscript support the intrinsic affinity between carboxylate groups and Au. In case of SAM formed at low pH via COO$^-$ adsorption, the symmetric stretching band was observed at 1370 cm^{-1} (Ref. 36), while in our case the position of band A is at around 1390 cm^{-1}, namely an intermediate position between adsorbed carboxylates and band B (i.e., free carboxylates of the more vertically oriented 4-MBA molecule). This is the concept that we wanted to articulate at pg. 8, when we stated that "These evidences strongly suggest that in the case of 4-MBA, the SERS intensity at around 1400 cm^{-1} is due to carboxylates groups differently bound to the metal surface, depending on pH". In our interpretation, the intensity around 1400 cm^{-1} is the convolution of bands A and B: both come from S-Au bonded deprotonated 4-MBA, but in band A the molecules are tilted and the COO$^-$ group may be affected by the gold surface. The following figure shows the SERS intensities collected from AuNP at pH 4.0, 6.4 and 7.4 in the range 625-785 cm^{-1}. The intensities were normalized using band C located at 1068 cm^{-1} (ν_{12} ring vibration).
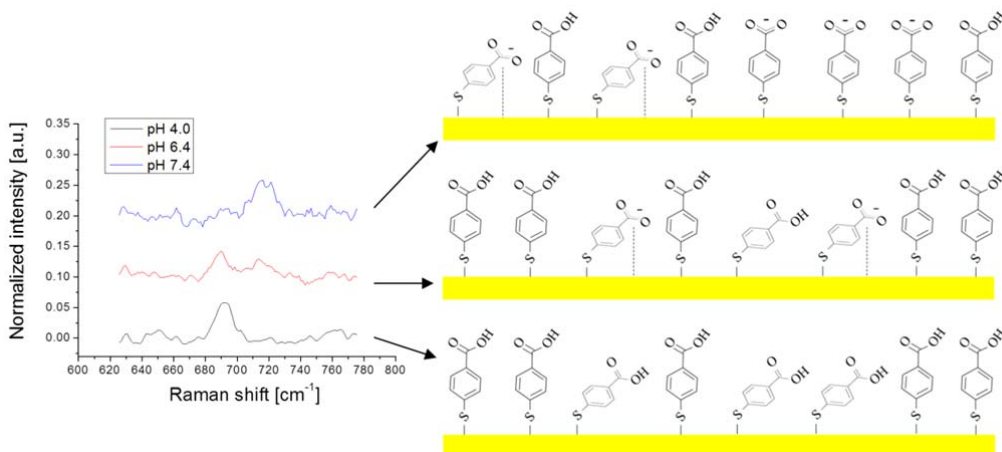
The bands at 694 and 720 cm^{-1} are assigned to out-of-plane γ(CCC) vibrations in acidic and neutral/alkaline environments, respectively (Phys Chem Chem Phys., 2015;17(39):26093-100. doi: 10.1039/c5cp03844h). From these data, as shown in the explanatory sketches of the figure, we inferred that some 4-MBA molecules of the SAM are tilted toward the gold surface (as also observed in other papers). The reduced distance between the gold surface and the carboxylates of the tilted 4-MBA molecules may explain the interaction causing stretching of the C-O bonds, namely redshift of the Raman frequencies associated to COO$^-$ symmetric stretching. Nonetheless, we agree that the conclusive clarification of the origin of band shift and asymmetry requires more investigation. The explanation of the COO$^-$ stretching band shift and asymmetry reported in previous studies is based on hydrogen bonding and the possible interaction between COO$^-$ groups and the ring hydrogens (Ref. 18, 22 and the new Ref. 35 of the second revised manuscript). This explanation makes sense and it also support the choice of the fitting procedure based on 2 bands, which is the focal point in our paper. Both bands are pH responsive. At acidic pH only Band A is observed and its intensity disappears at highly acidic pH. The latter evidence confirms that in the conjugated AuNP every 4-MBA molecule is pH responsive and there is no adsorption of COO$^-$ groups. The separation between band A and B becomes evident as pH rises to the alkaline range. Based on these considerations, we changed the text at the end of pg. 7: we removed the hypothesis of carboxylates-gold interaction and we reported only the intramonolayer hydrogen bonding between adjacent 4-MBA molecules. We removed the previous references 35 and 36. We added a new reference (Ref. 35 in the latest manuscript, Bishnoi, S. W. et al. All-optical nanoscale pH meter. Nano letters 6, 1687-1692 (2006)), which also reports asymmetry and shift of the band due to hydrogen bonding. Again, we thank the Reviewer for noticing this point in our discussion that may have been misleading.

Please note that the sentence "This reaction is favored at alkaline pH (i.e., pH>9 in our experiments), where the deprotonated 4-MBA is predominant and, consequently, the population of non-bonded −COO$^-$ groups increases along with the probability of plasmon-induced catalytic reaction forming CO$_2$ and TP" at pg. 9 of the first revised manuscript was replaced by "This reaction is favored at alkaline pH (i.e., pH>9 in our experiments), where the population of deprotonated 4-MBA increases along with the probability of plasmon-induced catalytic reaction forming CO$_2$ and TP" at the end of pg. 8 of the second revised manuscript.

Moreover, in line 6 of the paragraph *Outer cell membrane surface labelling* we changed "conjugate via carboxylate- and thiol-gold interactions" to "conjugate via thiol-gold interaction". In fact, the combination of "conjugate", "carboxylate" and "interactions" is misleading because the reader may infer that, in our SAM, COO$^-$ are adsorbed on the surface.

2.   Based on authors' assignment of 1370 cm-1 peak due to COO-Au, then these COO are not free, they can't respond to pH change, then they should not be counted in the intensity ratio (I_{A+B}/I_C) for the calibration curve. Did authors try to plot the calibration curve using I_B/I_C?

As stated in the answer to Comment 1, the intensity of band A responds to the variation of pH and it is undetectable at highly acidic pH. It implies that every COO$^-$ groups associated to this band are not adsorbed on the gold surface and they can be protonated. The plot of I_B/I_C is as follows:
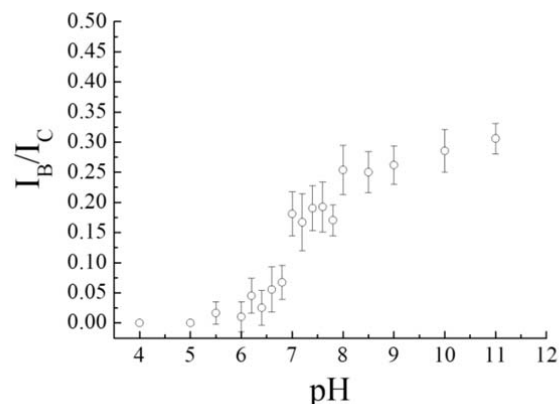
The data still show the typical trend of Henderson–Hasselbalch equation. We can notice a discontinuity at pH approaching 7.0. In fact, at more acidic pH the SERS intensity of the COO^- symmetric stretching is prevalently represented by band A.

Reviewer #3 (Remarks to the Author):

In this revised version of the manuscript the authors have performed significant improvements clarifying in a satisfactory way all the main issues pointed out by myself. In this respect they have clarified the important feature concerning the spatial resolution of the pH sensor and have also analysed the relevant reporter molecules that are used for pH estimation as well as performed an estimation of the SERS enhancemnet factor (lower bound). Therefore, I consider that the main concerns have adequately been answered and the manuscript is now suitable for publication in Nature Communications.

We thank the Reviewer for the positive comments and for her/his contribution throughout the entire revision process.

ADDITIONAL INFORMATION FROM THE AUTHORS:

At pg. 18, paragraph *Statistical analysis*, we changed "non-paired t-test" to "two-tailed unpaired t-test".

REVIEWERS' COMMENTS:

Reviewer #2 (Remarks to the Author):

In this second revision, authors have addressed my questions and comments in the first round review. I would recommend for publication in Nature Communications.